ORIGINAL RESEARCH

WILEY | BIOENERGY

Using dynamic relative climate impact curves to quantify the climate impact of bioenergy production systems over time

Sierk de Jong[1] (iD) | **Mark Staples[2]** | **Carla Grobler[2]** | **Vassilis Daioglou[3]** | **Robert Malina[2,4]** | **Steven Barrett[2]** | **Ric Hoefnagels[1]** | **André Faaij[5]** | **Martin Junginger[1]**

[1]Copernicus Institute of Sustainable Development, Utrecht University, Utrecht, The Netherlands

[2]Laboratory for Aviation and the Environment, Massachusetts Institute of Technology, Cambridge, Massachusetts

[3]Department of Climate, Air and Energy, PBL Netherlands Environmental Assessment Agency, The Hague, The Netherlands

[4]Center for Environmental Sciences, Hasselt University, Diepenbeek, Belgium

[5]Energy Academy Europe, University of Groningen, Groningen, The Netherlands

Correspondence
Sierk de Jong, Copernicus Institute of Sustainable Development, Utrecht University, Utrecht, The Netherlands.
Email: s.a.dejong@uu.nl

Abstract

The climate impact of bioenergy is commonly quantified in terms of CO_2 equivalents, using a fixed 100-year global warming potential as an equivalency metric. This method has been criticized for the inability to appropriately address emissions timing and the focus on a single impact metric, which may lead to inaccurate or incomplete quantification of the climate impact of bioenergy production. In this study, we introduce Dynamic Relative Climate Impact (DRCI) curves, a novel approach to visualize and quantify the climate impact of bioenergy systems over time. The DRCI approach offers the flexibility to analyze system performance for different value judgments regarding the impact category (e.g., emissions, radiative forcing, and temperature change), equivalency metric, and analytical time horizon. The DRCI curves constructed for fourteen bioenergy systems illustrate how value judgments affect the merit order of bioenergy systems, because they alter the importance of one-time (associated with land use change emissions) versus sustained (associated with carbon debt or foregone sequestration) emission fluxes and short- versus long-lived climate forcers. Best practices for bioenergy production (irrespective of value judgments) include high feedstock yields, high conversion efficiencies, and the application of carbon capture and storage. Furthermore, this study provides examples of production contexts in which the risk of land use change emissions, carbon debt, or foregone sequestration can be mitigated. For example, the risk of indirect land use change emissions can be mitigated by accompanying bioenergy production with increasing agricultural yields. Moreover, production contexts in which the counterfactual scenario yields immediate or additional climate impacts can provide significant climate benefits. This paper is accompanied by an Excel-based calculation tool to reproduce the calculation steps outlined in this paper and construct DRCI curves for bioenergy systems of choice.

KEYWORDS
bioenergy, biofuels, climate impact, climate mitigation, environmental performance, life-cycle assessment

1 | INTRODUCTION

Biomass is an important renewable energy source in climate change mitigation strategies, particularly for sectors relying on energy-dense liquid fuels, such as aviation, shipping, and long-haul trucking (Rose et al., 2014; World Wildlife Fund, 2011). The conventional approach to quantify the climate change mitigation value of bioenergy is based on cradle-to-grave life-cycle assessment (LCA) of greenhouse gas (GHG) emission fluxes (GHG-LCA), often using the 100-year global warming potential as an equivalency metric to convert non-CO_2 emissions into CO_2 equivalents (equivalency metrics are also commonly referred to as normalized (emission) metrics or characterization factors). This method is widely employed to compare system performance and to determine the compliance of bioenergy systems to sustainability standards or policies.

In the context of bioenergy, the conventional GHG-LCA approach is criticized for its treatment of time-dependent emission profiles and the related climate impacts (Cherubini, Bright, & Strømman, 2013; Daystar, Venditti, & Kelley, 2017; Kendall, Chang, & Sharpe, 2009; Levasseur et al., 2016; Levasseur, Lesage, Margni, Deschênes, & Samson, 2010; O'Hare et al., 2009). The net emission profile of bioenergy production is determined by (a) the cradle-to-grave life-cycle production emissions, (b) the displaced (fossil) emissions, (c) direct emissions from, for example, carbon stock changes in the feedstock production area, and (d) indirect emissions from market-mediated effects. Emission fluxes from the latter two effects are generally time-dependent, particularly when land clearing is involved (instigating land use change (LUC) emissions) and/or long-rotation feedstocks are used (e.g., forestry biomass; Cherubini, Bright, & Strømman, 2012; Cherubini, Peters, Berntsen, Strømman, & Hertwich, 2011; O'Hare et al., 2009; Porsö, Hammar, Nilsson, & Hansson, 2017; Zetterberg & Chen, 2015). These emission fluxes are measured against the initial carbon stocks or the carbon stocks in a counterfactual scenario in which no bioenergy is produced. The conventional GHG-LCA approach often employs linear amortization of carbon stock changes, measured relative to the initial carbon stocks, over an arbitrary production period (Kendall et al., 2009). Alternatively, a parity point can be calculated at which emissions of bioenergy production equal the emissions of the counterfactual scenario (Lamers & Junginger, 2013). However, both methods neglect the fact that the climate impact of GHGs increases with the atmospheric residence time and may therefore lead to incomplete conclusions about (relative) system performance and the timing of climate mitigation benefits (Cherubini et al., 2013; Daystar et al., 2017; Kendall et al., 2009; Levasseur et al., 2016, 2010 ; O'Hare et al., 2009). The use of discount rates (Hellweg, Hofstetter, & Hungerbuhler, 2003; Levasseur et al., 2010; O'Hare et al., 2009) and time correction factors (Kendall

et al., 2009; Schwietzke, Griffin, & Matthews, 2011) have been proposed; however, the former does not have a physical basis in climate science, and the latter is unable to consider prolonged temporal variability of emission profiles.

Moreover, the use of a single performance indicator, as defined by the impact category, equivalency metric, and analytical time horizon used in the conventional approach, does not reflect the complexity of the climate system (Cherubini et al., 2016). The climate impact can be quantified according to different impact categories along the cause-effect chain (i.e., GHG emissions, radiative forcing, temperature change, and climate damages) at or over different analytical time horizons for instantaneous and cumulative metrics, respectively (Cherubini et al., 2013, 2016 ; Levasseur et al., 2016). The impact categories exhibit different temporal responses to emission pulses, which affects the impact of emission timing (Cherubini et al., 2013; Kendall et al., 2009; O'Hare et al., 2009; Schwietzke et al., 2011). Similarly, the choice of equivalency metric affects the relative importance of short-lived to long-lived emission species (Cherubini et al., 2016). Additionally, the analytical time horizon determines the cutoff point of the analysis, thus excluding impacts beyond a certain time. The choice of performance indicator therefore contains a value judgment about the weighting of one-time versus sustained emission fluxes and short- versus long-lived climate forcers, and can thus benefit or disadvantage the evaluation of systems with a particular emission profile (IPCC, 2014).

Bioenergy systems demonstrate a wide variety of emission profiles, in terms of both emission species and timing. Therefore, it is necessary to appropriately treat time dependencies and value judgments in bioenergy GHG-LCA to be able to properly quantify and compare the performance of bioenergy systems. Various authors have proposed methods to incorporate one of the aforementioned aspects in LCA. Some studies focus on dynamic performance indicators to incorporate time-dependent emission profiles, such as the fuel warming potential (O'Hare et al., 2009), carbon neutrality factor (Schlamadinger, Spitzer, Kohlmaier, & Lüdeke, 1995; Zanchi, Pena, & Bird, 2012), or relative carbon indicator (Pingoud, Ekholm, Soimakallio, & Helin, 2016). Other authors have proposed alternative equivalency metrics, which vary in equivalency base, time horizon, and type of time horizon (time-dependent or fixed; Cherubini et al., 2013; Cherubini et al., 2016; Cherubini et al., 2012; Edwards & Trancik, 2014; Edwards, McNerney, & Trancik, 2016; Kendall, 2012; Levasseur et al., 2010; Peters, Aamaas, Marianne, Solli, & Fuglestvedt, 2011). In addition, several studies have quantified the performance of bioenergy systems for different impact categories, such as radiative forcing, temperature change, and economic damages (Ericsson et al., 2013; O'Hare et al., 2009; Porsö et al., 2017; Schwietzke et al., 2011; Withers, Malina, & Barrett, 2015; Zetterberg & Chen, 2015).

Building upon prior efforts, we aim to quantify the climate impact of bioenergy systems over time using Dynamic Relative Climate Impact (DRCI) curves. The DRCI quantifies the net climate impact of a production system relative to a fossil baseline over time. It is therefore not a climate impact category or equivalency metric (such as the global warming potential, GWP), but rather a means to express the climate impact of bioenergy systems over time *using* existing climate impact categories and equivalency metrics.

To the best of our knowledge, the DRCI approach is the first which enables consistent comparison of the climate impact of bioenergy systems with different time-dependent emission profiles, while offering the flexibility to compare the effects of value judgments regarding the impact category, analytical time horizon, and equivalency metric. The use of DRCI curves was illustrated for various bioenergy systems with different temporal emission profiles to study the impact of different emission profiles and value judgments. A reduced-order climate model was employed to translate emission profiles into impact categories and quantify the associated scientific uncertainty. This paper is accompanied by an Excel-based calculation tool (see Supporting Information Material), which allows users to reproduce the calculation steps outlined in this paper and construct DRCI curves based on emission profiles of a system of choice.

The remainder of this paper is structured as follows. Section 2 introduces the DRCI curves using a generalized approach and demonstrates the approach for three bioenergy systems. Section 3 discusses the DRCI results and quantifies the scientific uncertainty associated with climate impact modeling. Section 4 introduces variations on the three

bioenergy systems in scope to quantify the relative importance of emission sources (e.g., life-cycle emissions, LUC emissions, carbon debt, and foregone sequestration) and identify best practices for bioenergy production. Section 5 discusses the merits and limitations of the DRCI approach and the implications for the evaluation of bioenergy systems.

2 | MATERIALS AND METHODS

2.1 | Introducing dynamic relative climate impact curves

Table 1 provides an overview of existing impact indicators. In conventional GHG-LCA, the climate impact of bioenergy systems is often evaluated using the net GHG emission reduction or relative GHG emission reduction. The net GHG emission reduction is calculated by subtracting the life-cycle emissions of the bioenergy system (bio) by the emissions of a counterfactual scenario (cf). The latter includes life-cycle emissions of the displaced (fossil) product(s) and, if system expansion is used, potential co-products. The relative GHG emission reduction performance is quantified by dividing the net GHG emission reduction by the GHG of a fossil baseline, for example, electricity, diesel, or gasoline.

The Dynamic Relative Climate Impact (DRCI) was defined analogous to the relative GHG emission reduction (Equation (1)). The DRCI plotted over time (the "DRCI curve") quantifies the net climate impact of a production system relative to a fossil baseline over time. It is therefore not a climate impact category or equivalency metric (as extensively covered by others [Cherubini et al., 2013; Levasseur et

TABLE 1 Overview of impact indicators for bioenergy systems

Indicator	Equation	Impact category	Reference
Conventional GHG-LCA			
Net GHG emission reduction	$GHG_{bio} - GHG_{cf}$	GHG emissions	
Relative GHG emission reduction	$\frac{GHG_{bio} - GHG_{cf}}{GHG_{base}}$	GHG emissions	
This study			
Dynamic relative climate impact (DRCI)	$\frac{\text{Climate impact}_{bio}(t) - \text{Climate impact}_{cf}(t)}{\text{Climate impact}_{base}(t)}$	All climate impact categories	This study
Existing time-dependent performance indicators			
Carbon neutrality factor	$1 - \frac{\sum C_{bio}(t)}{\sum C_{cf}(t)}$	Carbon stock	Schlamadinger et al. (1995)
	$1 - \frac{\sum GHG_{bio}(t)}{\sum GHG_{cf}(t)}$	GHG emissions	Zanchi et al. (2012)
Carbon balance indicator	$\frac{\sum C_{bio}(t)}{\sum C_{cf}(t)/DF}$	Carbon stock	Pingoud et al. (2016)
Cumulative radiative forcing balance	$\frac{\sum RF_{bio}(t) - \sum RF_{cf}(t)}{\sum RF_{cf}(t)}$	Cumulative radiative forcing	Schwietzke et al. (2011)
Fuel warming potential	$\frac{\sum RF_{bio}(t)}{\sum RF_{cf}(t)}$	Cumulative radiative forcing	O'Hare et al. (2009)

Note. base: baseline scenario; bio: bioenergy scenario; cf: counterfactual scenario; DF: displacement factor, that is, units of fossil fuel displaced by one unit of biomass; GHG: greenhouse gas emissions; RF: radiative forcing.

The scope of emission species and fluxes covered in the counterfactual and bioenergy scenario may vary between authors.

al., 2016]), but rather a means to express the climate impact for bioenergy systems over time *using* existing climate impact categories and equivalency metrics.

$$\text{Dynamic Relative Climate Impact, DRCI}(t)$$
$$= \frac{\text{Climate impact}_{bio}(t) - \text{Climate impact}_{cf}(t)}{\text{Climate impact}_{base}(t)} \quad (1)$$

A negative DRCI value implies that the bioenergy scenario has a climate benefit over the counterfactual scenario. For example, an DRCI value of −0.5 indicates a 50% reduction in a particular impact category relative to the fossil baseline.

The relative formulation was selected over the net climate impact, as a dimensionless parameter allows for comparison between DRCI curves based on different impact categories. Moreover, the scientific uncertainty associated with climate models converges when the numerator and denominator in Equation (1) are of the same order of magnitude, since the uncertainty grows approximately proportional to the climate impact (see Section 3).

Unlike the indicators used in conventional GHG-LCA, the DRCI is time-dependent (dynamic) and thus requires the definition of an analytical time horizon at which the impact category is evaluated ($t = TH_a$). The choice of TH_a can be tailored to the aim of the analysis. Unlike previously proposed time-dependent performance indicators listed in Table 1 (O'Hare et al., 2009; Pingoud et al., 2016; Schlamadinger et al., 1995; Schwietzke et al., 2011; Zanchi et al., 2012), the DRCI definition allows for the use of different impact categories. Furthermore, it is defined relative to a fossil baseline instead of the counterfactual scenario to allow for comparison of production systems with different counterfactual scenarios. As such, the main value of the DRCI is that it is able to compare systems with varying temporal emission profiles and evaluate the effect of key value judgments regarding the time horizon, impact category, and equivalency metric.

In the following section, the DRCI curve approach will be demonstrated for three bioenergy systems with different temporal emission profiles to study the impact of different emission profiles and value judgments. The calculation steps are also featured in an Excel model which accompanies this paper (see Supporting Information Material).

2.2 | Demonstrating the DRCI curve approach for three bioenergy systems

The three bioenergy systems in scope were selected based on their distinct emission profile (Table 2). These systems are also featured in the calculation tool in the Supporting Information Material. The systems are stylized examples chosen to demonstrate the use of DRCI curves for systems with

TABLE 2 Characterization of the bioenergy systems in scope

System code	Bioenergy scenario Technology	Feedstock	Production location	Direct emissions	Indirect emissions	Counterfactual scenario	Fossil baseline
HEFA-UCO	Hydroprocessed esters and fatty acids	Used cooking oil	United States	Not applicable (residue from food industry)	None, as it was assumed no substitution effects take place	Aerobic digestion (without energy recovery) of disposed UCO (e.g., in the sewage system)	US diesel-type fossil fuels
FT-DWD	Gasification and Fischer–Tropsch synthesis	Downed woody debris (loblolly pine)	Eastern United States	Residue removal creates a carbon debt, fading over time as a new equilibrium is reached	None, as residues were not utilized before	Natural aerobic decay of downed woody debris	US diesel-type fossil fuels
ATJ-SC	Fermentation and Alcohol-to-Jet	Sugarcane	Brazil (grassy cerrado), imported to the United States	Carbon stock change due to land clearance and gradual loss of soil organic carbon	None, as virgin land is cleared	Foregone sequestration due to growth of natural vegetation	US diesel-type fossil fuels

different emission profiles, and therefore may contain simplifying assumptions and may be optimistic (e.g., UCO-HEFA) or pessimistic (e.g., ATJ-SC) compared to the most common biofuel production contexts. For example, the production contexts of the systems considered here were set such that no indirect emissions were induced, as quantifying indirect emissions over time requires economic modeling (e.g., general equilibrium modeling) and involves considerable uncertainties (Wicke, Verweij, van Meijl, van Vuuren, & Faaij, 2012). The selected systems produce 10 PJ/year middle-distillate (MD) transport fuels (gasoline, diesel, and/or jet fuel) on a commercial scale destined for the US market. The HEFA-UCO system is based on full hydrodeoxygenation of used cooking oil, a residue from the food industry. The FT-DWD system employs gasification and Fischer–Tropsch synthesis based on downed woody debris (DWD) from loblolly pine. The ATJ-SC system is based on the Alcohol-to-Jet technology, which converts alcohols (in this case sugarcane ethanol) to MD fuels through dehydration, oligomerization, and hydrogenation. Hydrogen consumption in the HEFA-UCO and ATJ-SC case is covered by steam methane reforming of natural gas.

2.3 | Dynamic life-cycle inventory

2.3.1 | Generalized approach

Given the DRCI is a time-dependent performance indicator, it requires a dynamic life-cycle inventory (LCI) which contains time-dependent inventory of emission fluxes, grouped by emission species (denoted with subscript i) (Daystar et al., 2017; Levasseur et al., 2010; O'Hare et al., 2009). A separate LCI exists for the bioenergy and counterfactual scenario, which represent alternative futures diverging from the production start year (t_0). The LCI is defined from t_0 to the LCI time horizon (TH_{LCI}) (O'Hare et al., 2009). If TH_{LCI} is longer than the production time horizon (TH_p), postproduction emission fluxes (e.g., regrowth) should be included.

The LCI of the bioenergy scenario (bio) consists of life-cycle production emissions ($Elc_{bio,i}$), direct emissions in the biomass production area ($Edir_{bio,i}$), and indirect emissions from market-mediated effects ($Eind_{bio,i}$) (Equation (2)). Direct emissions may include, for example, methane emissions from wetland drainage, or carbon stock changes from LUC or carbon debt. Indirect emissions may occur when increased crop production for bioenergy purposes affects global agricultural and fuel markets and instigates additional emissions in other sectors. Indirect LUC emissions are a prominent example of a market-mediated effect, whereby bioenergy production induces land conversion elsewhere, for example, due to increasing commodity prices. Biogenic combustion emissions in the bioenergy scenario should be included in Elc_i or be accounted for in $Edir_{bio,i}$ (i.e., adding the combustion emissions to the carbon sequestration due to feedstock growth).

The counterfactual scenario (cf) represents the anticipated future scenario in which no bioenergy is produced. It includes the life-cycle emissions of the main (fossil) products directly displaced by the produced quantity of bioenergy ($Edmp_{cf,i}$), direct emissions in the biomass production area ($Edir_{cf,i}$), and indirect emissions ($Eind_{cf,i}$) (Equation (3)). Direct emissions in the counterfactual scenario often involve foregone sequestration, which includes the future sequestration that would have occurred in the intended biomass production area if no bioenergy was produced. If system expansion is used, emissions from displaced co-products should also be considered in the counterfactual scenario ($Edcp_{cf,i}$). If mass, energy, or market value allocation is used for co-product allocation, this allocation procedure should also be applied to direct and indirect emissions in both scenarios (Cherubini et al., 2009).

System performance is often benchmarked against a fossil baseline to calculate the relative reduction and allow for comparison among systems. In biofuel regulation such as the US Renewable Fuel Standard 2 (RFS2) or EU Renewable Energy Directive (RED), the fossil baseline (or "fossil comparator") is often predefined based on average emission factors for a benchmark fossil product. In the current dynamic formulation, the fossil baseline is assumed constant over time and includes life-cycle emissions of the benchmark product ($Elc_{base,i}$) (Equation (4)).

$$LCI(t)_{bio,i} = Elc_{bio,i}(t) + Edir_{bio,i}(t) + Eind_{bio,i}(t) \qquad (2)$$

$$LCI(t)_{cf,i} = Edmp_{cf,i}(t) + Edcp_{cf,i}(t) + Edir_{cf,i}(t) + Eind_{cf,i}(t) \qquad (3)$$

$$LCI(t)_{base,i} = Elc_{base,i} \qquad (4)$$

In the formulation in Equations (2)–(4), sequestration is considered a negative emission. Unlike customary practice to allocate the difference in carbon stock between the bioenergy and counterfactual scenario entirely to the bioenergy scenario (see e.g., Zanchi et al.'s, 2012 carbon neutrality factor), the dynamic LCI presented above tracks actual emissions to the atmosphere in both scenarios. This distinction is required to calculate impact categories further down the cause-effect chain, due to the nonlinear relation between GHG emissions and these impacts.

2.3.2 | Dynamic life-cycle inventory for the bioenergy systems in scope

Based on Equations (2)–(4), a dynamic LCI was constructed for the bioenergy systems in scope. The LCI

comprised CO_2, CH_4, and N_2O emissions for the bioenergy and counterfactual scenarios and fossil baseline for $TH_p = TH_{LCI} = 100$ years (Figure 1 and Table 3). The emissions were summed by emission species and quantified per MJ of MD fuels. Biogenic emissions (from e.g., biomass or biofuel combustion) were assumed equal to the carbon sequestration from feedstock growth within the same year on a landscape level and were hence omitted from the LCI.

Life-cycle emissions and displaced emissions were calculated using the Greenhouse gases, Regulated Emissions and Energy use in Transportation model (GREET.net v.1.3.0.13107) (Argonne National Laboratory, 2018), using system expansion and cradle-to-grave supply chains described in de Jong et al. (2017). Life-cycle emissions were assumed constant over TH_p and TH_{LCI}. The fossil baseline was based on emission factors for diesel-type fuels as defined in the US RFS2 (US Environmental Protection Agency, 2010).

For simplicity, direct emissions were assumed to include carbon stock changes only. For the ATJ-SC system, carbon stock changes were modeled using the Lund-Potsdam-Jena with Managed Land (LPJml) model within the Integrated Model to Assess the Global Environment (IMAGE) (Supporting Information Material S1) (Daioglou et al., 2017). The model tracks changes in above- and belowground carbon, carbon in soil litter, and soil carbon. The analysis uses the yearly average carbon stock of the grassy cerrado grid cells in Brazil. The model was run from 2020 to 2100, after which carbon stocks were assumed to stabilize. The sugarcane bagasse was used to produce electricity and heat, while sugarcane straw was assumed to be burnt in the field (Han, Dunn, Cai, Elgowainy, & Michael, 2012). Sugarcane yield was obtained from the LPJml model and was kept constant at 2015 levels (199 GJ/ha). The irregular behavior of the emission curves in Figure 1 is a result of the interpolation of IMAGE results, which uses a 5-year time step. The initial spike in emissions in the bioenergy scenario is caused by LUC emissions from land clearing. The remainder of emissions is due to loss of soil organic carbon over time. The counterfactual scenario shows negative Edir emissions due to foregone sequestration, since it was assumed that carbon stocks were not yet in equilibrium at the start of the project.

The FT-DWD case used DWD from a loblolly pine forest in which carbon stocks were assumed in equilibrium on a landscape level, hence no carbon stock changes were considered in the counterfactual scenario. The removal of DWD in the bioenergy scenario causes a carbon debt relative to the counterfactual in which DWD is left to decay. The portion of remaining DWD in the counterfactual scenario was approximated using an exponential decay

function $Mass(t) = Mass_0 \exp(-kt)$, in which k equals the annual decay rate ($k = 0.041$ for loblolly pine) (Russell et al., 2014). The carbon debt over time due to continuous extraction was computed by the convolution of the yearly extraction rate and the decay function. The carbon content of DWD was assumed to be 50% of total mass and constant over time. It was further assumed that belowground carbon was not affected by the extraction of DWD and all carbon in the biomass decays as CO_2 (no CH_4 was produced). As shown in Figure 1, continuous extraction of DWD in the bioenergy scenario causes a large reduction in carbon stock initially, until a new equilibrium is reached after approximately 100 years.

2.4 | Quantifying the climate impact of emission profiles

2.4.1 | Generalized approach

The impact of GHG emissions on the earth's climate can be evaluated for different impact categories along the cause-effect chain (Figure 2). The emission of GHGs changes the atmospheric concentration of the respective species. GHGs are naturally removed from the atmosphere at a species-specific rate due to interactions with the atmospheric, terrestrial, and oceanic system. The emission concentration in the atmosphere instigates a net change in the energy balance of the earth system ("radiative forcing"), which consequently causes a change in global mean surface temperature ("temperature change"). The temperature response is delayed due to the inertia of the climate system (e.g., thermal inertia of oceans). Temperature change, in turn, may be related to impact categories such as sea level rise and welfare loss. Compared to other climate impact categories, GHG emissions are quantified with more certainty and regulated more easily. Moving down the cause-effect chain generally increases the policy relevance, but also increases the scientific uncertainty (Cherubini et al., 2013).

Conventional GHG-LCAs and parity point analyses generally evaluate system performance at the GHG emission level. The conversion of emission profiles to other impact categories can be done using complex climate models (Joos et al., 2013), reduced-order climate impact models (e.g., MAGICC (Meinshausen, Raper, & Wigley, 2011), ACC2 (Tanaka et al., 2007), or APMT-IC (Mahashabde et al., 2011; Wolfe, 2015)), or following simpler relationships between the indicators as demonstrated in the Excel model (see Supplementary Information Material) and described in various sources (Cherubini et al., 2013; Ericsson et al., 2013; Myhre & Shindell, 2014; O'Hare et al., 2009). Equivalency metrics are often used to translate the impact of non-CO_2 emissions into CO_2 equivalents.
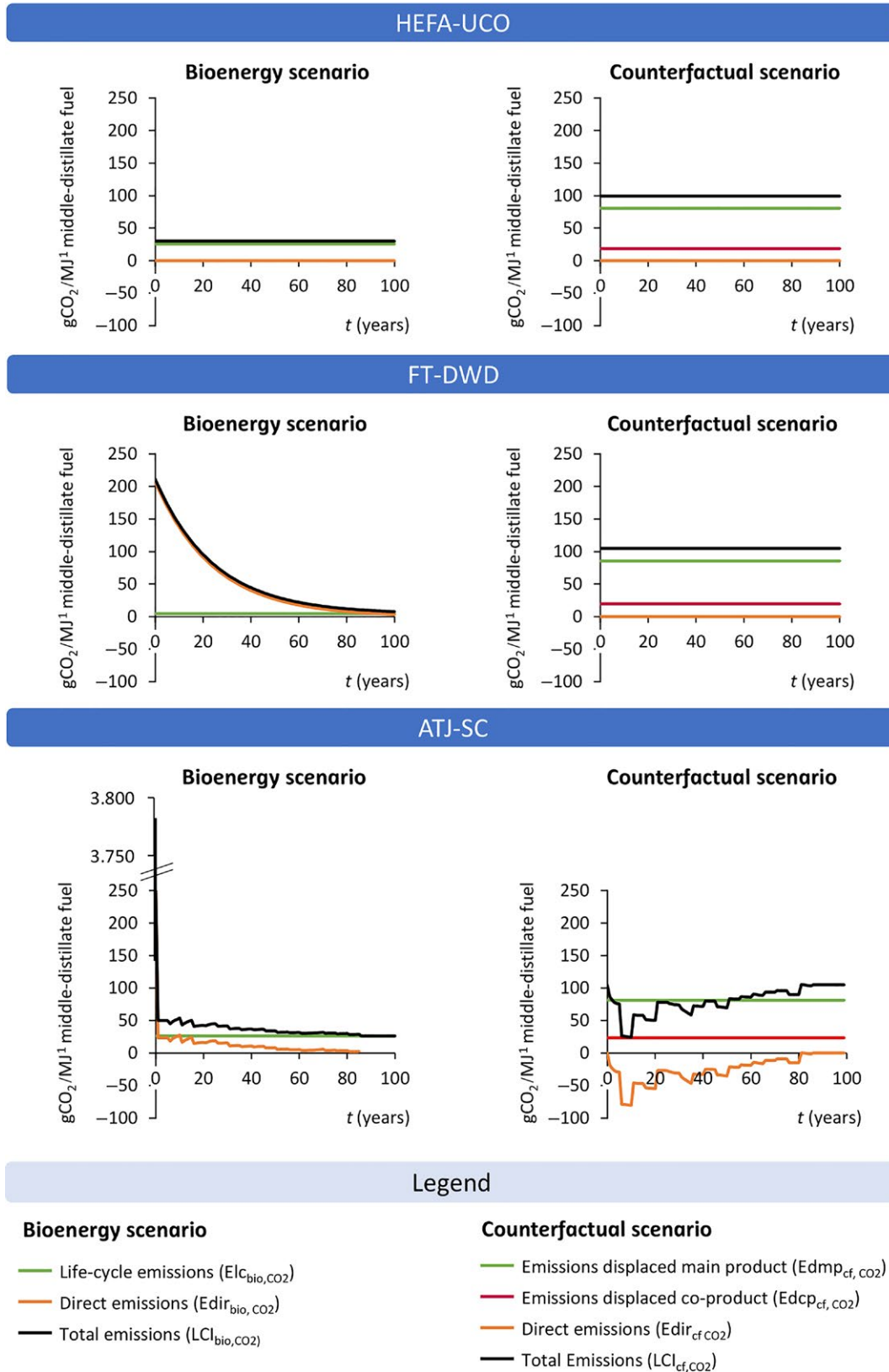
FIGURE 1 Dynamic LCI of three bioenergy systems in scope, showing instantaneous CO_2 emissions

Climate efficacies can be used to align the temperature response of species-induced radiative forcing (Cherubini et al., 2013).

As the climate response extends beyond the time of the emission discharge, it is required to define the analytical time horizon, TH_a, at which the impact category is evaluated. The

TABLE 3 LCI for CO_2, CH_4, and N_2O for three bioenergy systems

Scenario	Bioenergy	Counterfactual	Bioenergy	Counterfactual	Bioenergy	Counterfactual
$LCI_{CO_2}(t)$ (g/MJ_{MD})	30	99	Time-dependent (Figure 1)		Time-dependent (Figure 1)	89
$LCI_{CH_4}(t)$ (g/MJ_{MD})	0.12	0.19	0.020	0.22	0.20	0.20	0.094
$LCI_{N_2O}(t)$ (mg/MJ_{MD})	3.4	3.1	4.1	4.6	38	3.6	2.2
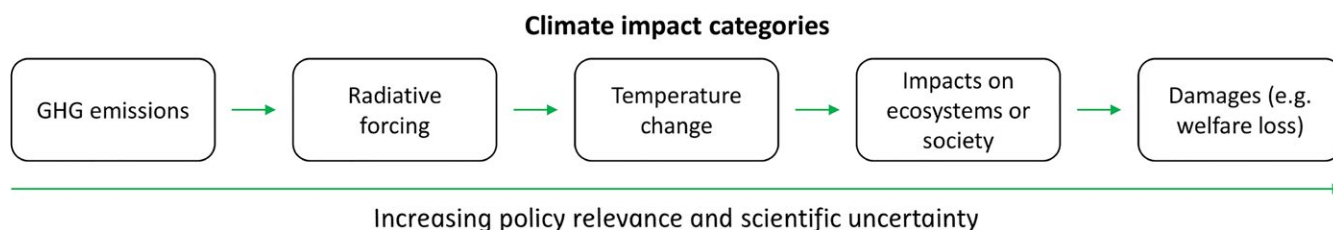
FIGURE 2 Cause-effect chain for GHG emissions (adapted from Cherubini et al., 2013)

TH_a often exceeds the production and LCI time horizon (TH_p and TH_{LCI}).

2.4.2 | Quantifying the climate impact of the bioenergy systems in scope

The climate module of the Aviation Environmental Portfolio Management Tool (referred to as APMT-Impacts Climate (APMT-IC)) was used to calculate impact categories from the dynamic LCIs described in Section 2.2. APMT-IC is a reduced-order climate model which models the physical and monetary impacts of CO_2, CH_4, N_2O, sulfates, soot, NO_x, and H_2O emissions. Although the toolset, its algorithm, and assumptions have been well documented and used in numerous previous studies (Barrett et al., 2012; Mahashabde et al., 2011; Stratton, Wolfe, & Hileman, 2011; Trivedi, Malina, & Barrett, 2015; Withers et al., 2015, 2014; Wolfe, 2012, 2015), it has recently undergone a number of updates to align with the state of the science. Therefore, the methods for APMT-IC used in this study are presented in the Supporting Information Material S3. For current purposes, the use of APMT-IC was confined to CO_2, CH_4, and N_2O emissions. The equivalency metrics to equate CO_2, CH_4, and N_2O emissions were calculated with APMT-IC. Climate efficacies were obtained from the Model for Assessment of Greenhouse Gas Induced Climate Change (MAGICC6) (Meinshausen et al., 2011). The model was run using an RCP 2.6 background emission scenario. The impact of using an RCP 8.5 scenario is discussed in Supporting Information Material S4.

The quantification of climate impacts beyond GHG emissions introduces scientific uncertainty related to climate impact modeling parameters, such as the climate sensitivity and radiative efficacies of emission species (Cherubini et al., 2013, 2016; Levasseur et al., 2016; Reisinger, Meinshausen, & Manning, 2011). APMT-IC

captures this type of uncertainty using Monte Carlo simulation, in which key model parameters were varied using predefined probabilistic distributions (Wolfe, 2015). The climate impact was calculated using the mean and 5th and 95th percentile results. For sake of clarity, only the mean values are shown in the results section; the associated uncertainty is addressed separately in Section 3.2.

2.5 | Quantifying the DRCI

2.5.1 | Generalized approach

The DRCI can be quantified for different impact categories and equivalency metrics. The choice of impact category affects the impact of emission timing, while the choice between cumulative and instantaneous impact categories affects the value of one-time versus sustained emissions (Cherubini et al., 2013; Kendall et al., 2009; O'Hare et al., 2009; Schwietzke et al., 2011). For example, cumulative impact categories generally respond more slowly to emission events compared to instantaneous impact categories, because they record all impacts over the analytical time horizon. The choice of equivalency metric affects the relative importance of short-lived to long-lived emission species (Cherubini et al., 2016). Due to the flexible formulation of the DRCI, it can be used to analyze the effect of these value judgments on the climate impact of bioenergy systems.

2.5.2 | Quantifying the DRCI of the bioenergy systems in scope

The DRCI curves for the three bioenergy systems were constructed for three existing climate impact categories, based on their distinct temporal response:

1. Cumulative emissions using a fixed GWP_{100} as an equivalency metric ($DRCI_{Em,cum}$),
2. Instantaneous radiative forcing using climate efficacies ($DRCI_{RF,inst}$),
3. Cumulative temperature change ($DRCI_{\Delta T,cum}$).

The change in instantaneous radiative forcing is faster than cumulative emissions, as it depends on emission concentrations which include emission decay mechanisms. Radiative forcing also responds faster than temperature change, as temperature response is delayed due to the inertia of the climate system (Withers et al., 2015).

A comparison of different equivalency metrics to compute $DRCI_{Em,cum}$ can be found in Supporting Information Material S2, as the effect on system performance was small compared to the choice of impact category and analytical time horizons.

3 | RESULTS

3.1 | Climate impact and analytical time horizon

Figure 3 shows the $DRCI_{Em,cum}$, $DRCI_{RF,inst}$, and $DRCI_{\Delta T,cum}$ for the three bioenergy systems in scope. The DRCI curves for HEFA-UCO are relatively constant over time and across the three impact categories, due to its stable emission profile. The DRCI curves for ATJ-SC start high initially ($DRCI_{Em,cum} = 39.6$), but decline rapidly as the impact of up-front LUC emissions fades over time. The FT-DWD system shows a steady decline, because the emission pulses associated with carbon debt are generally less irregular over time compared to initial LUC emissions. The DRCI curves start to stabilize after 100 years, as the TH_{LCI} is reached.

The choice of impact category affects observed system performance, particularly for systems with time-dependent emission profiles such as the ATJ-SC and FT-DWD systems. For example, the ATJ-SC system reduces instantaneous radiative forcing by 9% relative to the fossil baseline after 100 years, while it increases cumulative temperature change by 50% over the same analytical time horizon. Due to their distinct temporal response, the choice of impact category also alters the importance of one-time versus sustained emissions. Systems with large initial LUC emissions, such as ATJ-SC, yield lower DRCI values when evaluated based on instantaneous and rapidly responding impact categories (i.e., instantaneous radiative forcing), compared to cumulative and slowly responding impact categories (e.g., cumulative temperature change). This applies to a lesser extent to systems with sustained emissions (e.g., FT-DWD and HEFA-UCO), as their overall climate impact is less dependent on the weighting of one-time emission events. As a result, the choice of impact category affects the comparison between systems with one-time and sustained emissions.

As stipulated in prior analyses, the choice of impact category also affects the relative importance of short- and long-lived emission species (Cherubini et al., 2016; Levasseur et al., 2016). For example, instantaneous radiative forcing emphasizes the importance of short-lived forcers compared to cumulative emissions, especially in the first years. This effect is illustrated for FT-DWD by comparing $DRCI_{Em,cum}$ and $DRCI_{RF,inst}$ at $TH_A = 0$, at which the bioenergy scenario shows higher CO_2 emissions than the counterfactual, but lower CH_4 and N_2O emissions. As the $DRCI_{RF,inst}$ allocates a higher weighting to CH_4 and N_2O savings than the $DRCI_{Em,cum}$, the former is lower (0.80) than the latter (1.07). This effect is less prominent for HEFA-UCO, because
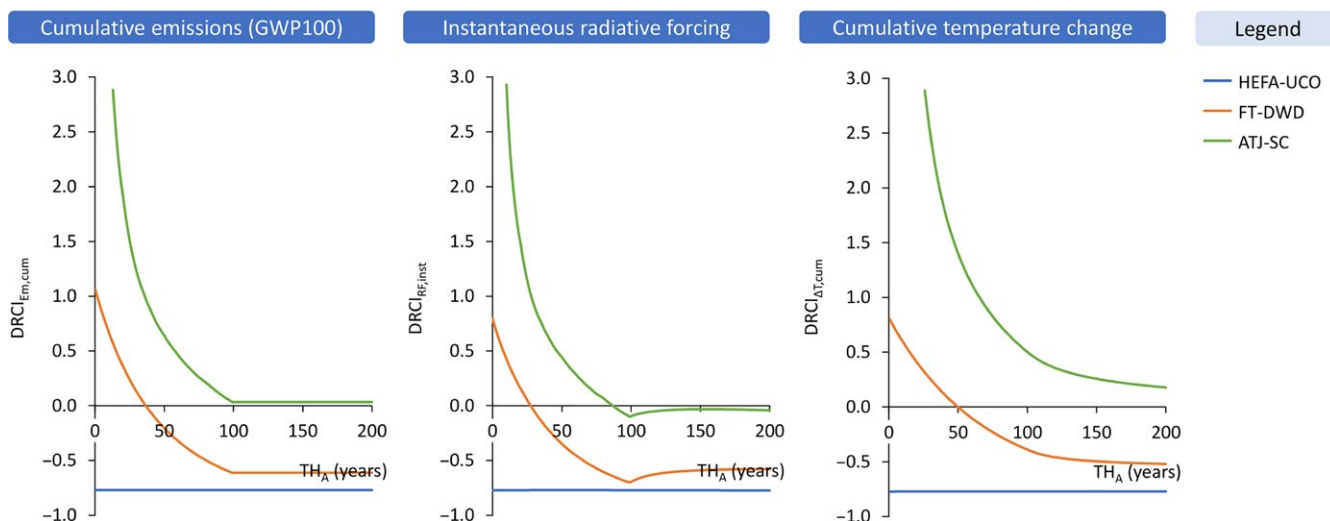
FIGURE 3 DRCI curves for three bioenergy systems for cumulative greenhouse gas emissions, instantaneous radiative forcing, and cumulative temperature change as a function of the analytical time horizon (TH_A)
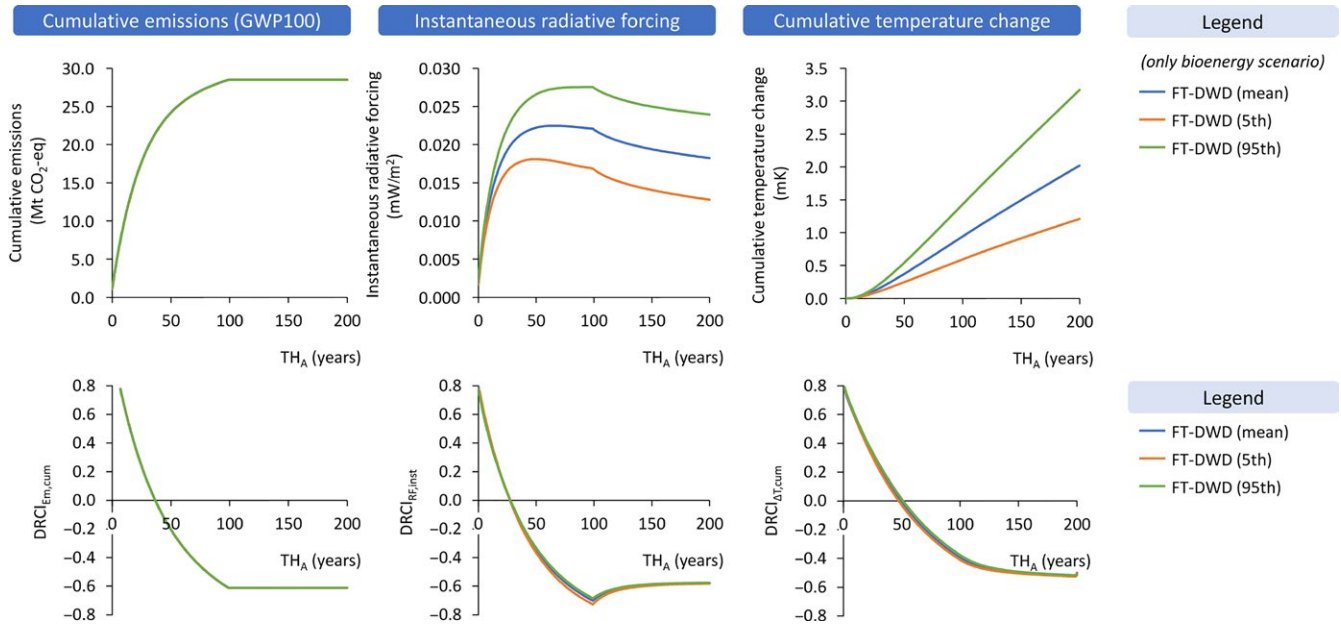
FIGURE 4 The scientific uncertainty associated with climate impact modeling for the FT-DWD system

amplification of CH_4 and N_2O emissions savings is counteracted by a decreased impact of CO_2 savings. The choice of equivalency metric also affects the relative importance of short- versus long-lived species, but has a smaller impact on overall system performance than the impact category and time horizon (Supporting Information Material S2).

3.2 | Scientific uncertainty

Figure 4 shows the 5th and 95th percentile results of APMT-IC for the FT-DWD system. For absolute climate impacts, the scientific uncertainty is substantial and grows over time; for example, for cumulative temperature change at $TH_A = 100$ years, the 5th and 95th percentile results range between −37% and +52% of the mean result. However, the uncertainty reduces to ±5% for the DRCI (i.e., relative to a fossil baseline), because the uncertainty in the numerator of the DRCI is paired with the uncertainty in the denominator and increases approximately proportionally. The uncertainty in the DRCI grows with increasing absolute difference between the numerator and the denominator (not with time), albeit marginally (the maximum uncertainty equaled ±10% for a dummy run in which the ratio between the numerator and the denominator was defined 100,000 times larger). Similar converging behavior has been observed for uncertainty related to different background emission concentration scenarios (Supporting Information Material S4). DRCI curves can therefore be used to study the effect of bioenergy production on a wide range of impact categories (with higher policy relevance) without dramatically increasing the uncertainty associated

with climate impact modeling and background emission concentration.

4 | VARIABILITY IN BIOENERGY SYSTEMS

This section evaluates alternative systems based on the FT-DWD and ATJ-SC systems to quantify the relative importance of emissions sources and identify best practices for bioenergy production. The analysis includes variations in life-cycle emissions, LUC emissions, carbon debt, and foregone sequestration. The fossil baseline remained the same throughout all analyses. The various systems are discussed in more detail in Supporting Information Material S1.

4.1 | FT-DWD

Four alternative systems were considered for FT-DWD:

- FT-DWD-CCS. This system applies carbon capture and storage (CCS), lowering life-cycle emissions by 108 gCO_2/MJ_{MD} (Kreutz, Larson, Liu, & Williams, 2008).
- FT-DWD-HighDecay and FT-DWD-LowDecay. These systems use DWD from tree species with the highest ($k = 0.076$; water oak) and lowest ($k = 0.023$; red pine) decay rates observed in Eastern US forests, which affects the overall carbon debt (Russell et al., 2014).
- FT-DWD-CFBurn. This system assumes a counterfactual
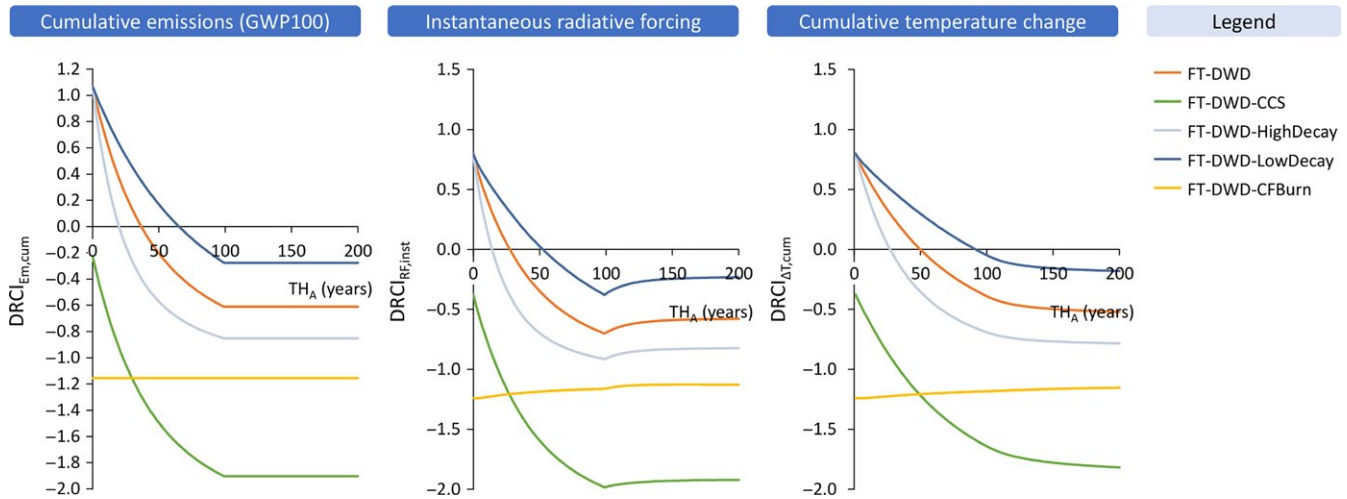
FIGURE 5 Alternative production systems based on FT-DWD

scenario in which the DWD is burnt in the forest without energy recovery, for example, to prevent forest fires. No carbon debt is included in the bioenergy scenario, because the biogenic carbon of the DWD is also released immediately in the counterfactual scenario.

The results shown in Figure 5 indicate that the application of CCS yields the lowest DRCI values after 27–49 years (depending on the impact category), as it offsets the carbon debt with carbon storage. The impact of carbon debt would not be visible in conventional GHG-LCA, as temporal emission fluxes (apart from LUC emissions) are usually not incorporated. However, the results show that the counterfactual scenario or selected tree species may affect system performance considerably, especially for shorter analytical time horizons. The spread in DRCI values as a result of different decay rates varies between -0.70 and 0.02 for $DRCI_{RF,inst}$ ($TH_A = 50$ years) and -0.35 and 0.30 for $DRCI_{\Delta T,cum}$ ($TH_A = 50$ years). The DRCI curve for the FT-DWD-CFBurn system is relatively constant and is less than -1 for all TH_A and impact categories, which means that it has a net negative climate impact.

4.2 | ATJ-SC

Seven alternative production systems were considered for ATJ-SC:

- ATJ-SC-CCS. This system applies CCS to the fermentation step, lowering life-cycle emissions by 27 gCO_2/MJ$_{MD}$ (Möllersten, Yan, & Jose, 2003).
- ATJ-SC-5th and ATJ-SC-95th. These systems cultivate sugarcane on Brazilian cerrado soils with low and high carbon stocks (the 5th and 95th percentile of the carbon stock distribution within the cerrado biome), leading to 0.1 and 2 times the LUC emissions compared to the mean (in terms of t CO_2/ha).

- ATJ-SC-TropicalForest and ATJ-SC-Abandoned. These systems assume cultivation of sugarcane on an average grid cell (in terms of carbon stock) in the tropical forests and abandoned agricultural land biomes. Whereas the former system instigates high initial LUC emissions, the latter system assumes significant amounts of foregone sequestration from regrowth of natural vegetation in the counterfactual scenario.
- ATJ-SC-LUCPrevention. This system assumes bioenergy production is accompanied by measures to prevent indirect LUC emissions (e.g., by increasing agricultural yields or improving supply chain efficiencies (Brinkman, Wicke, Gerssen-Gondelach, van der Laan, & Faaij, 2015)) such that additional sugarcane is produced on existing sugarcane land without increasing life-cycle emissions or causing direct or indirect LUC emissions. These measures are not implemented in the counterfactual scenario.
- ATJ-SC-ImprovedYield. This system assumes sugarcane yield on cerrado land improves to 2050 levels (266 GJ/ha), based on IMAGE-LPJml projections (Daioglou et al., 2017).

The results in Figure 6 indicate that a profound difference exists between converting low-carbon or high-carbon cerrado, for which DRCI values vary between -0.11 and 1.01 for $DRCI_{RF,inst}$ ($TH_A = 50$ years) and 0.20 and 2.85 for $DRCI_{\Delta T,cum}$ ($TH_A = 50$ years). The difference mainly originates from higher initial LUC emissions for the high-carbon cerrado case, which also explains the larger difference between the systems when evaluated using $DRCI_{\Delta T,cum}$.

Sugarcane cultivation on cerrado, abandoned agricultural land, or tropical forest shows comparable DRCI curves, because high LUC emissions are mitigated by high sugarcane yields (and vice versa). Furthermore, foregone sequestration creates a large carbon sink in the counterfactual scenario of the ATJ-SC-Abandoned system, leading to higher DRCI
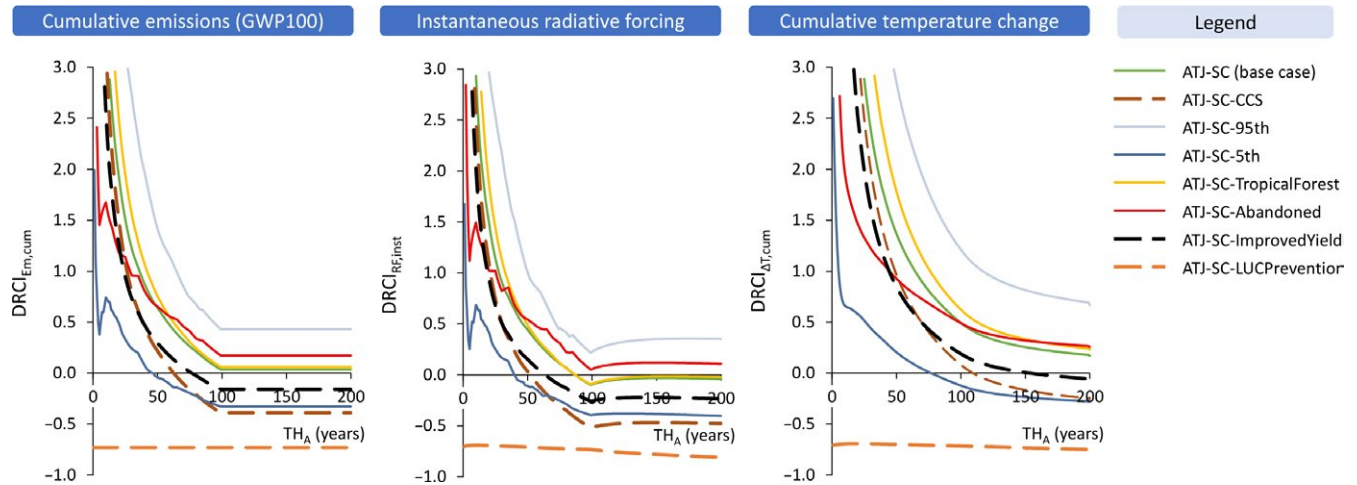
FIGURE 6 Alternative production systems based on ATJ-SC

values over longer time horizons. This effect is particularly apparent for $DRCI_{RF,inst}$; the ATJ-SC-Abandoned system initially has a lower DRCI values than ATJ-SC (base case) and ATJ-SC-TropicalForest due to low initial LUC emissions, but gradually shows a higher $DRCI_{RF,inst}$ due to foregone sequestration. This example also shows how the choice of performance metric may change the merit order of systems and why foregone sequestration effects are important when assessing system performance.

If LUC emissions can be prevented, DRCI values are reduced to approximately −0.7 across all impact categories and time horizons (ATJ-SC-LUCPrevention system). This underlines the importance of LUC prevention measures to achieve high climate impact reductions using bioenergy. The application of CCS shifts the $DRCI_{Em,cum}$ curve of the ATJ-SC system by −0.42 for all TH_A. Improvements in sugarcane yield reduce DRCI values particularly for short TH_A, as carbon stock changes (particularly initial LUC emissions) are lower because less land is required to produce the same quantity of biofuel.

5 | DISCUSSION

5.1 | The use of DRCI curves

DRCI curves are time-dependent and are able to incorporate the temporal emission profiles associated with LUC emissions, carbon debt, and foregone sequestration. Therefore, DRCI curves are suitable to analyze a wide array of bioenergy systems. It also allows for a transparent comparison of bioenergy systems using different impact categories (including equivalency metrics) and analytical time horizons. Due to its ratio formulation, it is relatively robust to scientific uncertainties in climate impact modeling and background emission concentration scenarios. An Excel-based calculation model

is provided in the Supplementary Information Material to reproduce the calculation steps outlined in this paper and construct DRCI curves for bioenergy systems of choice.

DRCI curves provide more flexibility than conventional performance indicators, such as the relative GHG emission reduction and carbon parity point, which are essentially one-dimensional in terms of the point of evaluation. The relative GHG emission reduction method often employs linear amortization of initial LUC emissions over an amortization period. This approach is mathematically equivalent to evaluating the DRCI for cumulative emissions at an analytical time horizon equal to the amortization period (e.g., 30 years), with the relevant exception that the DRCI formulation also includes emission fluxes beyond the first year of the project (e.g., from foregone sequestration). The carbon parity point is the analytical time horizon for which the DRCI for cumulative emissions equals zero. The DRCI can therefore be used for direct comparison between the relative GHG reduction, carbon parity point, and indicators using a different point of evaluation (Figure 7).

Moreover, DRCI curves can be used to illustrate how the choice of impact category and analytical time horizon alters the merit order of systems. For instance, the FT-DWD-HighDecay system has higher DRCI values than the HEFA-UCO system when evaluated using conventional indicators, while it has a lower $DRCI_{Em,cum}$ from 78 years onwards. The ATJ-SC-CCS and FT-DWD-LowDecay systems yield similar carbon parity points (63 and 66 years, respectively), while FT-DWD-LowDecay shows lower DRCI values for the first 147 years in terms of cumulative temperature change.

In addition, DRCI curves quantify the climate benefits of a system over time, which enables the definition of an "eligibility quadrant" (Figure 7a,b). The eligibility quadrant is a two-dimensional threshold which can be used to determine whether a bioenergy production system is below a maximum
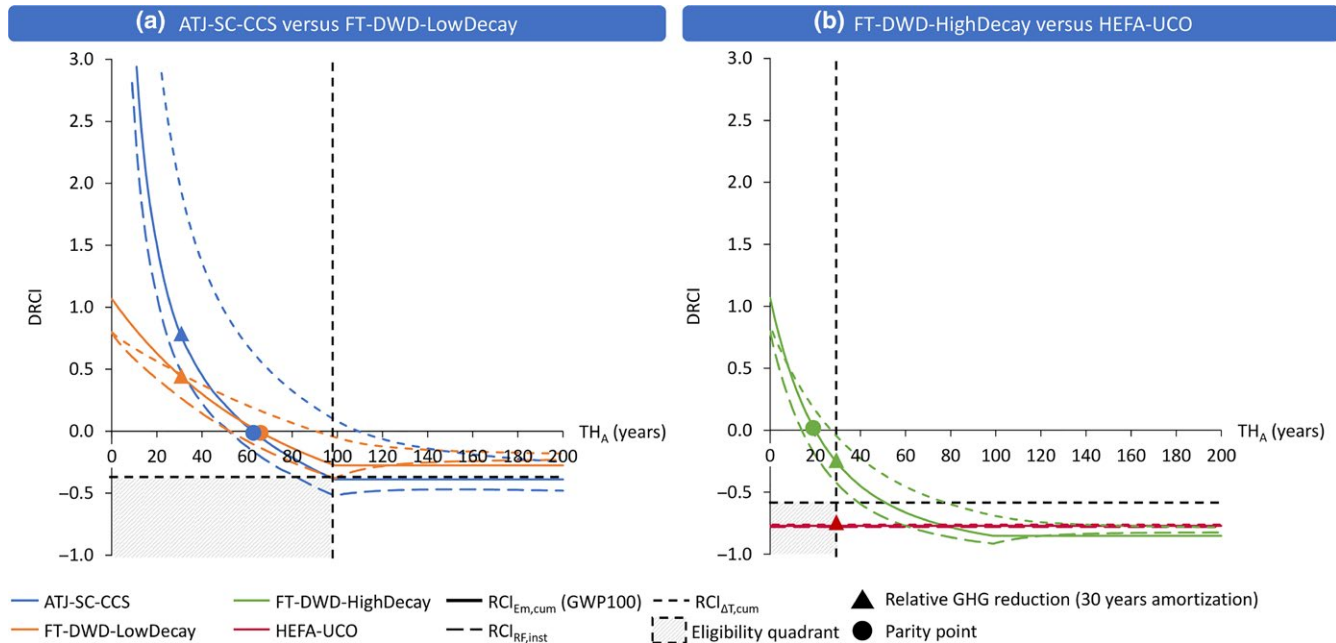
FIGURE 7 Comparison of DRCI curves with the relative GHG emission reduction (triangles; amortization period 30 years) and carbon parity point (circles). The eligibility quadrants were placed at a DRCI = −0.35 and TH_A = 100 years (left) and DRCI = −0.60 and TH_A = 30 years (right)

DRCI value before a given analytical time horizon, as defined by a policy or certification scheme of interest. The definition of these thresholds and the type of impact category they apply to have a significant impact on the eligibility of different bioenergy systems, especially those with time-dependent emission profiles. For instance, placing the eligibility quadrant at $DRCI_{Em,cum}$ = −0.35 and TH_A = 100 years would qualify ATJ-SC-CCS as eligible, while cumulative temperature is increased by 8% relative to the baseline (Figure 7a). Alternatively, the HEFA-UCO system is the only system meeting DRCI values below −0.6 before TH_A = 30 years, while the FT-DWD-HighDecay system has lower DRCI values over longer analytical time horizons for all impact categories (Figure 7b).

The choice of impact category, analytical time horizon, and equivalency metric is essentially a value judgment about the importance attributed to one-time (e.g., LUC emissions) versus sustained (e.g., carbon debt or foregone sequestration) emission fluxes and short- versus long-lived climate forcers. Similarly, the definition of the eligibility quadrant and the type of climate impact category required to meet the threshold are value judgments that should be made in accordance with the research or policy purpose. Shorter analytical time horizons allocate more weight to short-term emission events, while short analytical time horizons for equivalency metrics allocate more weight to short-lived climate forcers (Cherubini et al., 2016). Longer analytical and production time horizons will yield lower DRCI values, as the climate impact of the bioenergy systems in scope generally improves over time.

Cumulative impact categories keep memory of short-lived emission species and one-time emission pulses (e.g., from LUC), but are also criticized for not reflecting the actual climate response (Cherubini et al., 2013; Levasseur et al., 2016). The choice for instantaneous impact categories can be aligned with a peaking or stabilization year of the respective impact and may be well suited for goal-setting (Edwards & Trancik, 2014; Levasseur et al., 2016). Impact categories further down the cause-effect chain introduce a time lag in the analysis due to delayed climate response, but may be a better proxy for climate damages such as extreme weather events, sea level rise, and loss of permanent ice (Edwards & Trancik, 2014; Levasseur et al., 2016). Although the current study focused on midpoint impact categories, the DRCI curve approach may also be used for endpoint impact categories such as economic damage or sea level rise.

Besides bioenergy systems, DRCI curves can also be used to evaluate and compare other climate change mitigation measures, particularly those with time-dependent emission profiles and relatively large upfront emissions, such as electric vehicles, wind turbines, or solar panels.

5.2 | The limitations of DRCI curves

The flexibility of DRCI curves is a key strength; however, it should be calculated and applied consistently to allow for comparison between analyses. An Excel-based calculation model was added to the Supplementary Information Material to allow users to replicate the approach used in this study. The

DRCI value is a relative measure and therefore does not provide information on the absolute climate impact of a bioenergy system. Multiplication by the climate impact of the fossil baseline yields an estimate of the absolute climate impact; however, this comes with greater scientific uncertainty. The use of DRCI curves is particularly valuable for systems with time-dependent emission profiles. However, adequate quantification of direct and indirect emissions requires comprehensive models, which may complicate the practical implementation of the DRCI approach. Moreover, the definition of counterfactual scenarios is a delicate exercise, as it may have a significant impact on the results (as e.g., shown by FT-DWD-CFBurn).

The scope of climate forcers can be expanded to include surface albedo, surface roughness, evapotranspiration, and additional emissions species such as sulfates, soot, NO_x, and H_2O emissions (Cherubini et al., 2016). The impact of these effects may be of the same order of magnitude as GHG emission fluxes, either in a positive or negative direction (Caiazzo et al., 2014; Simmons & Matthews, 2016). Several of these issues require climate models with higher spatial and temporal resolution than those used in this study, especially because the location and timing of direct and indirect effects may vary between the bioenergy and counterfactual scenario.

5.3 | Implications for bioenergy production systems

The impact of LUC emissions, carbon debt, and foregone sequestration on the performance of bioenergy systems is significant and may in some cases exceed the impact of life-cycle emissions (Fargione, Hill, Tilman, Polasky, & Hawthorne, 2008; Searchinger et al., 2008; Valin et al., 2015). Feedstock–technology systems with high feedstock yields and conversion efficiencies mitigate the contribution of LUC emissions, carbon debt, and foregone sequestration, while the application of CCS can reduce the life-cycle emissions significantly.

The occurrence of LUC emissions, carbon debt, or foregone sequestration is driven by the production context rather than the feedstock–technology combination. The production contexts of the analyzed bioenergy systems were intentionally framed to contain these types of emissions for the sole purpose of demonstrating the impact of temporal emission profiles. These systems should therefore not be interpreted as typical bioenergy system with the most probable counterfactual scenario.

Direct LUC emissions can be reduced by producing bioenergy feedstocks on low carbon stock soils. The risk of indirect LUC emissions and carbon debt can be mitigated by shaping the right production context, for instance, by supplementing bioenergy production with efforts to optimize land/forest management, improve agricultural yields, increase supply chain efficiencies, and integrate bioenergy,

food, and feed production (Brinkman, Wicke, & Faaij, 2017; Gerssen-Gondelach, Wicke, Borzęcka-Walker, Pudełko, & Faaij, 2016; Jonker, Junginger, & Faaij, 2014; Peters et al., 2016; van de Staai et al., 2012; Wicke et al., 2012). The Shared Socioeconomic Pathways 1 (SSP 1) scenario represents such a storyline, in which land use for biomass production increases alongside a reduction in land use for food production caused by high agricultural yield improvements, changing food consumption patterns and low population growth (Doelman et al., 2018). Furthermore, production contexts in which the counterfactual scenario yields immediate or additional climate impacts (e.g., burning of forestry residues to prevent forest fires) can yield highly negative DRCI values. As DRCI curves incorporate these time-dependent emission fluxes, it is a valuable approach to select production contexts in which bioenergy systems consistently show a climate benefit, as shown, for example, in the ATJ-SC-LUCPrevention and FT-DWD-CFBurn systems.

The importance of time-dependent emission fluxes and the production context suggests that bioenergy GHG-LCAs and bioenergy policy frameworks should move beyond the static characterization of the cradle-to-grave life-cycle emissions of feedstock–technology combinations, toward a time-dependent characterization of the bioenergy production context, including carbon stock changes, (in)direct LUC emissions, realistic counterfactual scenario(s), and time-dependent parameters such as feedstock yield or carbon intensities of fossil products. The predictive character of such analysis introduces additional uncertainties that should be addressed appropriately, for example, by scenario analysis or using probability distributions (Supporting Information Material S5 discusses the issue of the potential and likelihood of bioenergy systems).

This analysis further demonstrates the importance of evaluating bioenergy system performance using different impact categories and analytical time horizons, which particularly applies to systems with time-dependent emission profiles. For example, the impact of initial LUC emissions on system performance will be greater when considering cumulative and slowly responding impact categories or shorter analytical time horizons. We found that the choice of equivalency metric did not significantly affect the DRCI value for the bioenergy systems in scope, but can be important when a large difference in non-CO_2 emissions exists between the bioenergy and counterfactual scenario (Supporting Information Material S2). This may apply to systems associated with high fertilizer use (emitting N_2O), methane leakage (e.g., biogas), or peatland conversion (emitting CH_4).

ORCID

Sierk de Jong https://orcid.org/0000-0002-8110-4527

REFERENCES

Argonne National Laboratory. (2018). Greenhouse Gases, Regulated Emissions, and Energy Use in Transportation (GREET) GREET.net Computer Model. Retrieved April 1, 2018, from https://greet.es.anl.gov/index.php?content=greetdotnet

Barrett, S. R. H., Yim, S. H. L., Gilmore, C. K., Murray, L. T., Kuhn, S. R., Tai, A. P. K., … Waitz, I. A. (2012). Public health, climate, and economic impacts of desulfurizing jet fuel. *Environmental Science and Technology*, *46*, 4275–4282. https://doi.org/10.1021/es203325a

Brinkman, M. L. J., Wicke, S. J., Gerssen-Gondelach, Carina, van der Laan, A. P. C., & Faaij (2015). *Methodology for assessing and quantifying ILUC prevention options*. Retrieved from https://www.uu.nl/sites/default/files/20150106-iluc_methodology_report.pdf

Brinkman, M. L. J., Wicke, B., & Faaij, A. P. C. (2017). Low-ILUC-risk ethanol from Hungarian maize. *Biomass and Bioenergy*, *99*, 57–68. https://doi.org/10.1016/j.biombioe.2017.02.006

Caiazzo, F., Malina, R., Staples, M. D., Wolfe, P. J., Yim, S. H. L., & Barrett, S. R. H. (2014). Quantifying the climate impacts of albedo changes due to biofuel production: A comparison with biogeochemical effects. *Environmental Research Letters*, 9. https://doi.org/10.1088/1748-9326/9/2/024015

Cherubini, F., Bird, N. D., Cowie, A., Jungmeier, G., Schlamadinger, B., & Woess-Gallasch, S. (2009). Energy- and greenhouse gas-based LCA of biofuel and bioenergy systems: Key issues, ranges and recommendations. *Resources, Conservation and Recycling*, *53*, 434–447. https://doi.org/10.1016/j.resconrec.2009.03.013

Cherubini, F., Bright, R. M., & Strømman, A. H. (2012). Site-specific global warming potentials of biogenic CO_2 for bioenergy: Contributions from carbon fluxes and albedo dynamics. *Environmental Research Letters*, *7*, 045902.

Cherubini, F., Bright, R. M., & Strømman, A. H. (2013). Global climate impacts of forest bioenergy: What, when and how to measure? *Environmental Research Letters*, *8*, 014049.

Cherubini, F., Fuglestvedt, J., Gasser, T., Reisinger, A., Cavalett, O., Huijbregts, M. A. J., … Levasseur, A. (2016). Bridging the gap between impact assessment methods and climate science. *Environmental Science & Policy*, *64*, 129–140. https://doi.org/10.1016/j.envsci.2016.06.019

Cherubini, F., Peters, G. P., Berntsen, T., Strømman, A. H., & Hertwich, E. (2011). CO_2 emissions from biomass combustion for bioenergy: Atmospheric decay and contribution to global warming. *GCB Bioenergy*, *3*, 413–426. https://doi.org/10.1111/j.1757-1707.2011.01102.x

Daioglou, V., Doelman, J. C., Stehfest, E., Müller, C., Wicke, B., Faaij, A., & van Vuuren, D. P. (2017). Greenhouse gas emission-curves for advanced biofuel supply chains. *Nature Climate Change*, *7*, 920–924. https://doi.org/10.1038/s41558-017-0006-8

Daystar, J., Venditti, R., & Kelley, S. S. (2017). Dynamic greenhouse gas accounting for cellulosic biofuels: Implications of time based methodology decisions. *International Journal of Life Cycle Assessment*, *22*, 812–826. https://doi.org/10.1007/s11367-016-1184-8

deJong, S., Antonissen, K., Hoefnagels, R., Lonza, L., Wang, M., … Junginger, M. (2017). Life-cycle analysis of greenhouse gas emissions from renewable jet fuel production. *Biotechnology for Biofuels*, *10*, 1–18. https://doi.org/10.1186/s13068-017-0739-7

Doelman, J. C., Stehfest, E., Tabeau, A., van Meijl, H., Lassaletta, L., Gernaat, D. E. H. J., … van Vuuren, D. P. (2018). Exploring SSP land-use dynamics using the IMAGE model: Regional and gridded scenarios of land-use change and land-based climate change mitigation. *Global Environmental Change*, *48*, 119–135. https://doi.org/10.1016/j.gloenvcha.2017.11.014

Edwards, M. R., McNerney, J., & Trancik, J. E. (2016). Testing emissions equivalency metrics against climate policy goals. *Environmental Science and Policy*, *66*, 191–198. https://doi.org/10.1016/j.envsci.2016.08.013

Edwards, M. R., & Trancik, J. E. (2014). Climate impacts of energy technologies depend on emissions timing. *Nature Climate Change*, *4*, 347–352. https://doi.org/10.1038/nclimate2204

Ericsson, N., Porsö, C., Ahlgren, S., Nordberg, Å., Sundberg, C., & Hansson, P.-A. (2013). Time-dependent climate impact of a bioenergy system – Methodology development and application to Swedish conditions. *GCB Bioenergy*, *5*, 580–590. https://doi.org/10.1111/gcbb.12031

Fargione, J., Hill, J., Tilman, D., Polasky, S., & Hawthorne, P. (2008). Land clearing and the biofuel carbon debt. *Science*, *319*, 1235–1238. https://doi.org/10.1126/science.1152747

Gerssen-Gondelach, S. J., Wicke, B., Borzęcka-Walker, M., Pudełko, R., & Faaij, A. P. C. (2016). Bioethanol potential from miscanthus with low ILUC risk in the province of Lublin, Poland. *GCB Bioenergy*, *8*, 909–924. https://doi.org/10.1111/gcbb.12306

Han, J., Dunn, J. B., Cai, H., Elgowainy, A., & Michael, W. Q. (2012). *Updated sugarcane parameters in GREET1_2012*, Second Revision. Retrieved from https://greet.es.anl.gov/files/greet-updated-sugarcane

Hellweg, S., Hofstetter, T. B., & Hungerbuhler, K. (2003). Discounting and the environment – Should current impacts be weighted differently than impacts harming future generations? *International Journal of Life Cycle Assessment*, *8*, 8–18.

IPCC (2014). *Climate change 2014 synthesis report. Contribution of Working Groups I, II and III to the Fifth Assessment Report of the Intergovernmental Panel on Climate Change*. https://doi.org/10.1017/CBO9781107415324.

Jonker, J. G. G., Junginger, M., & Faaij, A. (2014). Carbon payback period and carbon offset parity point of wood pellet production in the South-eastern United States. *GCB Bioenergy*, *6*, 371–389. https://doi.org/10.1111/gcbb.12056

Joos, F., Roth, R., Fuglestvedt, J. S., Peters, G. P., Enting, I. G., von Bloh, W., … Weaver, A. J. (2013). Carbon dioxide and climate impulse response functions for the computation of greenhouse gas metrics: A multi-model analysis. *Atmospheric Chemistry and Physics*, *13*, 2793–2825. https://doi.org/10.5194/acp-13-2793-2013

Kendall, A. (2012). Time-adjusted global warming potentials for LCA and carbon footprints. *International Journal of Life Cycle Assessment*, *17*, 1042–1049. https://doi.org/10.1007/s11367-012-0436-5

Kendall, A., Chang, B., & Sharpe, B. (2009). Accounting for time-dependent effects in biofuel life cycle greenhouse gas emissions calculations. *Environmental Science and Technology*, *43*, 7142–7147. https://doi.org/10.1021/es900529u

Kreutz, T. G., Larson, E. D., Liu, G., & Williams, R. H. (2008). Fischer-Tropsch fuels from coal and biomass. In *25th Annual International Pittsburgh Coal Conference* (pp. 1–81).

Lamers, P., & Junginger, M. (2013). The 'debt' is in the detail: A synthesis of recent temporal forest carbon analyses on woody biomass for energy. *Biofuels, Bioproducts and Biorefining*, *7*, 373–385.

Levasseur, A., Cavalett, O., Fuglestvedt, J. S., Gasser, T., Johansson, D. J. A., Jørgensen, S. V., … Cherubini, F. (2016). Enhancing life cycle impact assessment from climate science: Review of recent findings and recommendations for application to LCA. *Ecological Indicators*, *71*, 163–174. https://doi.org/10.1016/j.ecolind.2016.06.049

Levasseur, A., Lesage, P., Margni, M., Deschênes, L., & Samson, R. (2010). Considering time in LCA: Dynamic LCA and its application to global warming impact assessments. *Environmental Science and Technology*, *44*, 3169–3174. https://doi.org/10.1021/es9030003

Mahashabde, A., Wolfe, P., Ashok, A., Dorbian, C., He, Q., Fan, A., … Waitz, I. A. (2011). Assessing the environmental impacts of aircraft noise and emissions. *Progress in Aerospace Sciences*, *47*, 15–52. https://doi.org/10.1016/j.paerosci.2010.04.003

Meinshausen, M., Raper, S. C. B., & Wigley, T. M. l. (2011). Emulating coupled atmosphere-ocean and carbon cycle models with a simpler model, MAGICC6 – Part 1: Model description and calibration. *Atmospheric Chemistry and Physics*, *11*, 1417–1456. https://doi.org/10.5194/acp-11-1417-2011

Möllersten, K., Yan, J., & Jose, R. M. (2003). Potential market niches for biomass energy with CO_2 capture and storage – Opportunities for energy supply with negative CO_2 emissions. *Biomass and Bioenergy*, *25*, 273–285. https://doi.org/10.1016/S0961-9534(03)00013-8

Myhre, G., & Shindell, D. (2014). Anthropogenic and natural radiative forcing supplementary material. In: Climate Change 2013: The Physical Science Basis. Contribution of Working Group I to the Fifth Assessment Report of the Intergovernmental Panel on Climate Change. Retrieved from https://doi.org/10.1017/CBO9781107415324.018

O'Hare, M., Plevin, R. J., Martin, J. I., Jones, A. D., Kendall, A., & Hopson, E. (2009). Proper accounting for time increases crop-based biofuels' greenhouse gas deficit versus petroleum. *Environmental Research Letters*, *4*. https://doi.org/10.1088/1748-9326/4/2/024001

Peters, G. P., Aamaas, B., Marianne, T. L., Solli, C., & Fuglestvedt, J. S. (2011). Alternative "global warming" metrics in life cycle assessment: A case study with existing transportation data. *Environmental Science and Technology*, *45*, 8633–8641. https://doi.org/10.1021/es200627s

Peters, D., Spöttle, H., Thomas, K., Ann-Kathrin, C., Maarten, S., Tjeerd, J., … Grass, M. (2016). *Methodologies for the identification and certification of Low ILUC risk biofuels*. Retrieved from https://ec.europa.eu/energy/sites/ener/files/documents/ecofys_methodologies_for_low_iluc_risk_biofuels_for_publication.pdf

Pingoud, K., Ekholm, T., Soimakallio, S., & Helin, T. (2016). Carbon balance indicator for forest bioenergy scenarios. *GCB Bioenergy*, *8*, 171–182. https://doi.org/10.1111/gcbb.12253

Porsö, C., Hammar, T., Nilsson, D., & Hansson, P.-A. (2017). Time-dependent climate impact and energy efficiency of internationally traded non-torrefied and torrefied wood pellets from logging residues. *Bioenergy Research*, *11*, 1–13.

Reisinger, A., Meinshausen, M., & Manning, M. (2011). Future changes in global warming potentials under representative concentration pathways. *Environmental Research Letters*, *6*(2), 024020. https://doi.org/10.1088/1748-9326/6/2/024020

Rose, S. K., Kriegler, E., Bibas, R., Calvin, K., Popp, A., van Vuuren, D. P., & Weyant, J. (2014). Bioenergy in energy transformation and climate management. *Climatic Change*, *123*, 477–493. https://doi.org/10.1007/s10584-013-0965-3

Russell, M. B., Woodall, C. W., Fraver, S., D'Amato, A. W., Domke, G. M., & Skog, K. E. (2014). Residence times and decay rates of downed woody debris biomass/carbon in eastern US forests. *Ecosystems*, *17*, 765–777. https://doi.org/10.1007/s10021-014-9757-5

Schlamadinger, B., Spitzer, J., Kohlmaier, G. H., & Lüdeke, M. (1995). Carbon balance of bioenergy from logging residues. *Biomass and Bioenergy*, *8*, 221–234. https://doi.org/10.1016/0961-9534(95)00020-8

Schwietzke, S., Griffin, W. M., & Matthews, H. S. (2011). Relevance of emissions timing in biofuel greenhouse gases and climate impacts. *Environmental Science and Technology*, *45*, 8197–8203. https://doi.org/10.1021/es2016236

Searchinger, T., Heimlich, R., Houghton, R. A., Dong, F., Elobeid, A., Fabiosa, J., … Yu, T.-H. (2008). Use of U.S. croplands for biofuels increases greenhouse gases through emissions from land-use change. *Science*, *319*, 1238–1240. https://doi.org/10.1126/science.1151861

Simmons, C. T., & Matthews, H. D. (2016). Assessing the implications of human land-use change for the transient climate response to cumulative carbon emissions. *Environmental Research Letters*, *11*, 035001. https://doi.org/10.1088/1748-9326/11/3/035001

Stratton, R. W., Wolfe, P. J., & Hileman, J. I. (2011). Impact of aviation non-CO_2 combustion effects on the environmental feasibility of alternative jet fuels. *Environmental Science & Technology*, *45*, 10736–10743.

Tanaka, K., Kriegler, E., Bruckner, T., Hooss, G., Knorr, W., & Raddatz, T. (2007). *Aggregated Carbon cycle, atmospheric chemistry and climate model (ACC2): description of forward and inverse mode*. Retrieved from https://pubman.mpdl.mpg.de/pubman/faces/viewItemOverviewPage.jsp?itemId=escidoc:994422:1

Trivedi, P., Malina, R., & Barrett, S. R. H. (2015). Environmental and economic tradeoffs of using corn stover for liquid fuels and power production. *Energy & Environmental Science*, *8*, 1428–1437. https://doi.org/10.1039/C5EE00153F

US Environmental Protection Agency. (2010). Renewable Fuel Standard Program (RFS2) Regulatory Impact Analysis. Program, 1109.

Valin, H., Peters, D., van denBerg, M., Frank, S., Havlik, P., & Forsell, N. (2015). *The land use change impact of biofuels consumed in the EU - Quantification of area and greenhouse gas impacts (GLOBIOM report)*. Retrieved from https://ec.europa.eu/energy/sites/ener/files/documents/Final Report_GLOBIOM_publication.pdf

van de Staai, J., Peters, D., Dehue, B., Mayer, S., Schueler, V., Toop, G., …Laszlo, M. (2012). *Low Indirect Impact Biofuel (LIIB) methodology*. Retrieved from https://www.ecofys.com/files/files/12-09-03-liib-methodology-version-0-july-2012.pdf

Wicke, B., Verweij, P., van Meijl, H., van Vuuren, D. P., & Faaij, A. P. C. (2012). Indirect land use change: Review of existing models and strategies for mitigation. *Biofuels*, *3*, 87–100. https://doi.org/10.4155/bfs.11.154

Withers, M. R., Malina, R., & Barrett, S. R. H. (2015). Carbon, climate, and economic breakeven times for biofuel from woody biomass from managed forests. *Ecological Economics*, *112*, 45–52. https://doi.org/10.1016/j.ecolecon.2015.02.004

Withers, M. R., Malina, R., Gilmore, C. K., Gibbs, J. M., Trigg, C., Wolfe, P. J., … Barrett, S. R. H. (2014). Economic and environmental assessment of liquefied natural gas as a supplemental aircraft fuel. *Progress in Aerospace Sciences*, *66*, 17–36. https://doi.org/10.1016/j.paerosci.2013.12.002

Wolfe, P. J. (2012). *Aviation environmental policy effects on national- and regional- scale air quality, noise, and climate impacts* (Master thesis). Massachusetts Institute of Technology. Retrieved from https://dspace.mit.edu/handle/1721.1/71505

Wolfe, P. J. (2015). *Aviation environmental policy and issues of timescale*. Massachusetts Institute of Technology. Retrieved from https://hdl.handle.net/1721.1/101493

World Wildlife Fund (2011). *The Energy Report - 100% renewable energy by 2050*. Retrieved from https://c402277.ssl.cf1.rackcdn.com/publications/384/files/original/The_Energy_Report.pdf?1345748859

Zanchi, G., Pena, N., & Bird, N. (2012). Is woody bioenergy carbon neutral? A comparative assessment of emissions from consumption of woody bioenergy and fossil fuel. *GCB Bioenergy*, *4*, 761–772. https://doi.org/10.1111/j.1757-1707.2011.01149.x

Zetterberg, L., & Chen, D. (2015). The time aspect of bioenergy – Climate impacts of solid biofuels due to carbon dynamics. *GCB Bioenergy*, *7*, 785–796. https://doi.org/10.1111/gcbb.12174

SUPPORTING INFORMATION

Additional supporting information may be found online in the Supporting Information section at the end of the article.